Clays and Clay Minerals, Vol. 52, No. 1, 40–46, 2004.

PREPARATION AND CHARACTERIZATION OF L-ASPARTIC ACID-INTERCALATED LAYERED DOUBLE HYDROXIDE

QI YUAN[1], MIN WEI[1], ZHIQIANG WANG[2], GE WANG[1] AND XUE DUAN[1,*]

[1] Key Laboratory of Science and Technology of Controllable Chemical Reactions, Ministry of Education, Beijing University of Chemical Technology, Beijing 100029, PR China
[2] Department of Chemistry, Tsinghua University, Beijing 100084, PR China

Abstract—L-aspartic acid was intercalated into layered double hydroxides by coprecipitation. Two types of well crystallized material were obtained and were characterized by powder X-ray diffraction, Fourier transform infrared spectroscopy, thermogravimetry, differential thermal analysis and polarimetry. Schematic models of two intercalation structures with different basal spacings are given. It is proved that the optical activity of L-aspartic acid is retained during and after the intercalation process.

Key Words—Chiral Molecule, Coprecipitation, L-aspartic Acid, Layered Double Hydroxides, Intercalation.

INTRODUCTION

A key feature of the chemistry of layered material is the location of guest molecules of interest within the relatively constrained interlayer region. The incorporation of guest molecules into layered hosts is a versatile means by which to obtain novel nanocomposite materials. Layered double hydroxides (LDHs) were discovered in 1842 in Sweden but the first exact formula was not published until 1919 by Manasse. These materials can be represented by the general formula $[M^{2+}_{1-x}M^{3+}_{x}(OH)_2]^{x+}(A^{n-})_{x/n}\cdot mH_2O$, with which it is possible to synthesize hydrotalcites with different metal cations and anions.

The structure of LDH was disproved by Allmann and Taylor who carried out single-crystal X-ray diffraction (XRD) studies (Allmann, 1968; Ingram and Taylor, 1967), and showed that the structure may be described by considering the structure of brucite, $Mg(OH)_2$, which consists of charge-neutral sheets of edge-sharing hydroxide octahedra which form infinite sheets, with Mg^{2+} cations occupying the octahedral vacancies in the close-packed configuration of the OH^- ions. These sheets are stacked on top of each other and are held together by hydrogen bonding. In LDH, isomorphous substitution of a fraction of the Mg^{2+} cations with the trivalent cations (*e.g.* Al^{3+}) occurs and generates a positive charge on the layers which needs to be compensated by the CO_3^{2-} anions in order to balance the positive charge. Water of crystallization also occupies the free interlayer space of LDH. The hydroxyls in brucite-like sheets are tied to the CO_3^{2-} groups by the electrostatic force of attraction directly or via intermediate H_2O through hydrogen. The water molecules are loosely bound to the hydroxyl groups, and can be removed without destroying the structure (Kathleen *et al.*, 1988; Toshiyuki *et al.*, 1995).

With positively charged LDH structures, various anionic species have been intercalated into the gallery region of LDH layers mainly by coprecipitation or ion exchange, *e.g.* organic carboxylic acid (Stecher *et al.*, 1998; Oriakhi *et al.*, 1996), Keggin ions (Dimotakis and Pinnavaia, 1990), cyclodextrin (Zhao and Vance, 1997; Zhao and Vance, 1998), organic phosphoric acid (Nijis *et al.*, 1998), anionic polymer (Moujahid *et al.*, 2002; Oriakhi *et al.*, 1997), porphyrins (Tagaya *et al.*, 1996), and drugs (Ambrogi *et al.*, 2001). As a result, LDHs are now well established as excellent anion-exchange materials and their extensive intercalation chemistry has widespread applications in areas such as heterogeneous catalysis (Constantino and Pinnavaia 1994; Corma *et al.*, 1995), optical materials (Ogawa and Kuroda, 1995; Tagaya *et al.*, 1994), biomimetic catalysis (Sels *et al.*, 1999; Ukrainczyk *et al.*, 1995), and separation science (Fogg *et al.*, 1998, 1999).

Remarkable advances have been made in recent decades in the research of chiral technology due to its functional importance in the biological field and potential applications in the fields of functional materials (Andersson *et al.*, 1995). The common feature of amino acids is that they are all chiral molecules. There have been some reports on the intercalation of amino acids into LDHs, *e.g.* glutamic acid (Whilton *et al.*, 1997), tyrosine (Fudala *et al.*, 1999a, 1999b), and phenylalanine (Aisawa *et al.*, 2001). Whilton *et al.* (1997) intercalated aspartic acid and polyaspartic acid into LDH with a single basal spacing. However, studies on the relationship between anion orientation and its valence as well as the optical activity of intercalated chiral amino acid have not been reported. In the present work, L-aspartic acid (referred to hereafter as L-Asp) LDHs with two kinds of basal spacing were synthesized and explained. Moreover, the optical activity of L-Asp

* E-mail address of corresponding author:
duanx@mail.buct.edu.cn
DOI: 10.1346/CCMN.2004.0520105

Copyright © 2004, The Clay Minerals Society

https://doi.org/10.1346/CCMN.2004.0520105 Published online by Cambridge University Press

was retained after intercalation. Because some chiral substances such as drugs and biological molecules are unstable and may easily racemize under variant conditions, their reservoir charge is very high. Therefore, there is a potential application for regarding layered double hydroxides as 'molecule containers' to deposit and transport unstable chiral molecules.

EXPERIMENTAL

Synthesis

Mg-Al-CO_3^{2-} LDH was synthesized with separate nucleation and ageing steps (Zhao *et al*., 2002). Solution A, $Mg(NO_3)_2{\cdot}6H_2O$ and $Al(NO_3)_3{\cdot}9H_2O$ with a Mg^{2+}/Al^{3+} molar ratio of 2.0, were dissolved in deionized water. Solution B, NaOH and Na_2CO_3, were dissolved in deionized water to form the mixed alkalic solution. Solutions A and B were added simultaneously to a colloid mill rotating at 3000 rpm, and stirred for 2 min. The slurry obtained was removed from the colloid mill and heated at 100ºC for 6 h. The resulting solid was filtered, washed thoroughly with deionized water, and dried at 100ºC for 24 h.

Two L-Asp LDHs with different basal spacings were synthesized by coprecipitation via the following steps:

Sample 1: The molar ratio of $Mg^{2+}/Al^{3+}/OH^-$/L-Asp was 2.0/1.0/6.8/1.0. A solution of $Mg(NO_3)_2{\cdot}6H_2O$ and $Al(NO_3)_3{\cdot}9H_2O$ in deionized water was slowly added dropwise to a solution of NaOH and L-Asp with vigorous agitation under nitrogen atmosphere. The value of the pH at the end of addition was 10.0. After addition, the reaction mixture was heated at 100ºC for 6 h, washed with hot deionized water and dried at 70ºC for 18 h.

Sample 2: The same procedure as in sample 1 was followed except the molar ratio of $Mg^{2+}/Al^{3+}/OH^-$/L-Asp was 2.0/1.0/8.2/1.0, and after addition, 5 mol/L of NaOH were used to adjust the pH of the mixture to be 12.5.

Measurement of optical activity

The L-Asp and L-Asp LDHs (0.01 mol) were dissolved in HNO_3 (1:1, v/v) respectively, and the volume was fixed at 30 mL. The optical activity was measured at room temperature with a 10 cm sample tube.

Characterization

Powder X-ray diffraction (XRD) measurements were performed on a Rigaku XRD-6000 diffractometer, using CuKα radiation (λ = 0.154 nm) at 40 kV, 30 mA and a scanning rate of 0.02º/s from 3–70º2θ.

Fourier transform infrared (FTIR) spectra were recorded using a Vector22 (Bruker) spectrophotometer in the range 4000–400 cm^{-1} with 2 cm^{-1} resolution. The standard KBr disk (1 mg of sample in 100 mg of KBr) was used.

Thermogravimetric analysis and differential thermal analyses (TG-DTA) were performed on a PCT-1A thermal analysis system at a heating rate of 10ºC/min.

Elemental analysis was performed with a Shimadzu ICPS-7500 instrument. The C, H and N contents were determined using an Elementarvario elemental analysis instrument.

Optical rotation was carried out on a WZZ-1S automatic polarimetry at 589.3 nm (Na-D-line).

RESULTS AND DISCUSSION

The crystalline structure of L-Asp LDHs

The powder XRD patterns of the Mg-Al-CO_3^{2-} LDH, Sample 1 and Sample 2 are shown in Figure 1. The main diffraction peaks of Sample 1 with LDH structure appear at 9.51º (003), 19.5º (006) and 61.1º (110) (Figure 1b). The 003, 006, 009 and 110 peaks of Sample 2 are observed at 7.13, 14.0, 21.9 and 60.9º, respectively. The XRD pattern for the L-Asp LDHs would appear to exhibit the characteristic reflections of LDH materials with a series of 00*l* peaks, corresponding to the basal spacing, but for the organic derivative compounds, as is often the case (Bonnet *et al*., 1996), several of the 00*l* reflections disappear or broaden and the intensity of reflections decreased slightly compared with Mg-Al-CO_3^{2-} LDH. The basal spacing values of Sample 1 and Sample 2 are both different from that reported by Whilton *et al.* (1997), which will be discussed further below. There is a weak peak at 19.6º in Sample 2 (Figure 1c), which might be due to the co-intercalated nitrate ions within the gallery spaces (006 reflection for pure Mg-Al-NO_3^- LDH). For Sample 1 (Figure 1b), however, the characteristic peak of nitrate ions might be overlapped by the L-Asp anions. This shows that although an increase of the basal spacing is observed in the two cases when the carbonate anion is replaced by L-Asp, a few nitrate anions may also exist within the

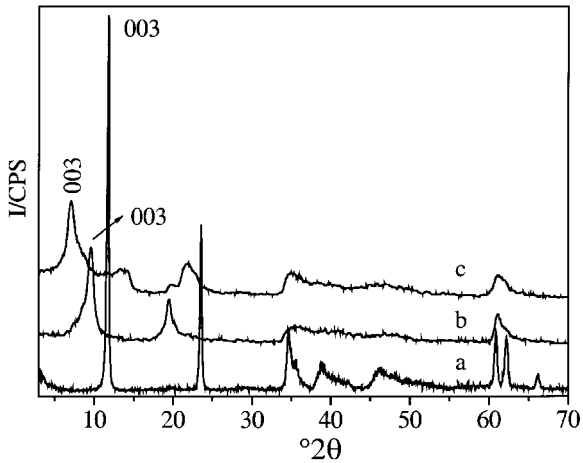


Figure 1. Powder XRD patterns of (a) Mg-Al-CO_3^{2-} LDH, (b) Sample 1 and (c) Sample 2.

https://doi.org/10.1346/CCMN.2004.0520105 Published online by Cambridge University Press

Table 1. Indexing the XRD patterns for Mg-Al-CO_3^{2-} LDH and L-Asp LDHs under different experimental conditions.

LDHs	Mg-Al-CO_3^{2-} LDH	Sample 1	Sample 2
d_{003} (nm)	0.758	0.929	1.238
d_{006} (nm)	0.379	0.456	0.634
d_{009} (nm)	0.259	0.258	0.406
d_{110} (nm)	0.152	0.152	0.152
$W_{1/2}$ for [003] (°)	0.026	0.094	0.114
$W_{1/2}$ for [110] (°)	0.034	0.084	0.064
Lattice parameter a (nm)	0.304	0.304	0.304
Lattice parameter c (nm)	2.293	2.615	3.724

layer of LDH. A similar phenomenon was found by Whilton *et al.* (1997).

Table 1 lists the basal spacing and lattice parameters for Mg-Al-CO_3^{2-} LDH and the two kinds of intercalation products. Apparently, the values of lattice parameter a of all three products are the same, 0.304 nm. This is because the value of a, which is related only to the atomic radius and composition of the 003 reflection, indicates the atomic density of the 003 reflection. The same elements and similar composition (see the elemental analysis part) in the host layer of the three products gives rise to the same lattice parameter a. However, the values of lattice parameter c for the three products are quite different. It is known that the value of c relates to the size and orientation of the gallery anion. Moreover, we note that the parameter a which has been calculated with d_{110} may be not accurate enough because the 110 reflections which shifted a little to a higher angle are affected by the broadening of both the 110 and 112 reflections.

IR spectroscopy

The FTIR spectra of the Mg-Al-CO_3^{2-} LDH, L-Asp and L-Asp LDHs are presented in Figure 2. The strong absorption at 3020 cm^{-1} seen in Figure 2d, along with several weak absorptions in the range 3050–2200 cm^{-1} is assigned to the N–H asymmetric vibration stretching of L-Asp. The broad bands around 3443 cm^{-1} (Figure 2a), 3453 cm^{-1} (Figure 2b) and 3455 cm^{-1} (Figure 2c), correspond to the O–H stretching vibration of surface and interlayer water of LDHs, which are at a lower frequency region than O–H in free water, at 3600 cm^{-1}. This is attributed to the formation of hydrogen bonds between interlayer water and different guest anions as well as the hydroxide groups of the layers. The asymmetric and symmetric stretching vibrations of alkyl carboxylic groups are observed at 1585–1395 cm^{-1} (Figure 2b), and at 1590–1385 cm^{-1} (Figure 2c), respectively. Compared with carboxylic acid (~1700 cm^{-1} and 1500 cm^{-1}), both of the peaks of the carboxylic groups shifted to the low frequency. The difference between the asymmetric and symmetric stretching vibration frequencies ($\Delta\nu$ values are 190 cm^{-1} and 205 cm^{-1}, respectively) provides information about the symmetry of the interaction between the carboxylate group and the hydroxylated layers, which is similar to salt-like compounds (Nakamoto, 1997; Prevot *et al.*, 1998). Additionally, the difference between the two $\Delta\nu$ values of Sample 1 and Sample 2 might indicate that there is some difference in the interaction of two intercalated samples between guest anions and host layers, which relates to the different anion states and orientation of interlayer guests. This will be discussed in the following section. The absorption band of co-intercalated NO_3^- (~1385 cm^{-1}) might be overlapped by that of symmetric stretching vibration of R–COO^-. Moreover, the weak bands at 2987 cm^{-1} (Figure 2b) and at 2997 cm^{-1} (Figure 2c) corresponding to the asymmetric C–H stretching vibration confirm the intercalation of L-Asp into the LDH. The lattice vibration of metal cations Al^{3+} and Mg^{2+} are noted at 790 cm^{-1} and 667 cm^{-1} (Figure 2a), at 777cm^{-1} and 667 cm^{-1} (Figure 2b), and at 776 cm^{-1} and 663 cm^{-1} (Figure 2c). In addition, the absorption bands at 554 cm^{-1} and 451 cm^{-1} (Figure 2a), at 555 cm^{-1} and 449 cm^{-1} (Figure 2b), and at 556 cm^{-1} and 448 cm^{-1} (Figure 2c) are assigned to the M–O–M and O–M–O skeletal stretching and bending vibrations.

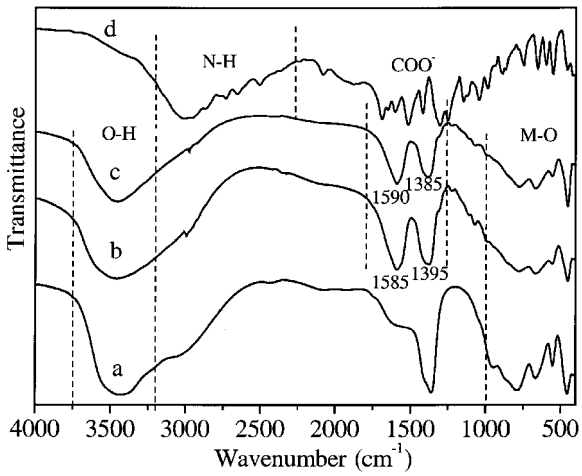


Figure 2. FTIR spectra of (a) Mg-Al-CO_3^{2-} LDH, (b) Sample 1, (c) Sample 2 and (d) L-Asp.

https://doi.org/10.1346/CCMN.2004.0520105 Published online by Cambridge University Press

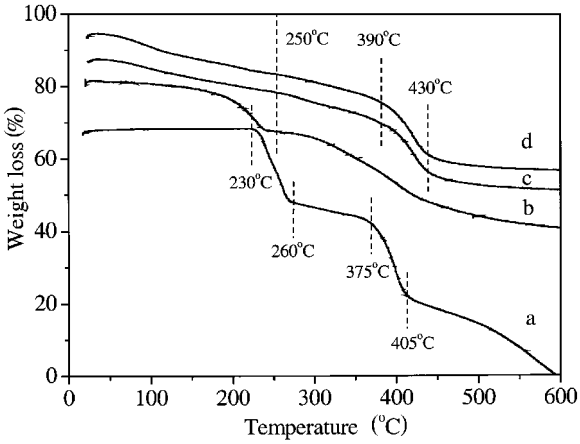


Figure 3. TG curves of (a) L-Asp, (b) Mg-Al-CO_3^{2-} LDH, (c) Sample 1 and (d) Sample 2.

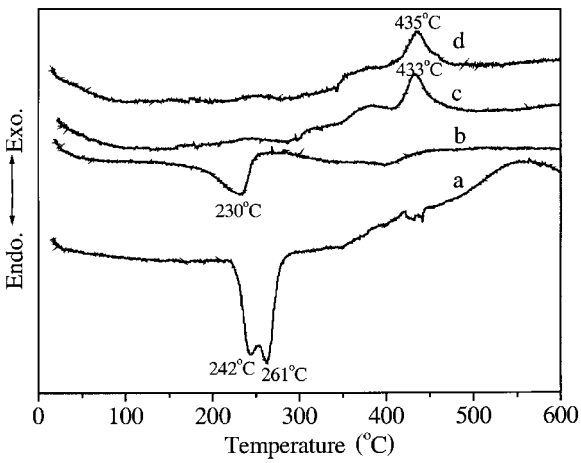


Figure 4. DTA curves of (a) L-Asp, (b) Mg-Al-CO_3^{2-} LDH, (c) Sample 1 and (d) Sample 2.

TG and DTA analysis

The TG and DTA curves of the L-Asp, Mg-Al-CO_3^{2-} LDH and L-Asp LDHs are shown in Figures 3 and 4, respectively. In the case of L-Asp as a reference sample (Figure 3a), a sharp weight loss in the temperature range 230–260ºC (25 wt.%) is due to the polymerization of L-Asp (Whilton *et al.*, 1997), which corresponds to the endothermic peak in Figure 4a. The second weight loss between 375 and 405ºC (22 wt.%) attributed to the decomposition as well as the combustion of L-Asp, relates to the mild exothermic peak in Figure 4a, as a result of the reverse and comparative thermal effect. The thermal decomposition of the Mg-Al-CO_3^{2-} LDH is characterized by two steps: the first from room temperature to 250ºC corresponds to the removal of surface water (from both the internal gallery surface and the external surface); the second, in the temperature region 250–450ºC (28 wt.%), is due to dehydroxylation of the brucite-like sheets as well as decomposition of the carbonate anions. The TG/DTA curves of Sample 1 (Figure 3c and Figure 4c) and Sample 2 (Figure 3d and Figure 4d) are rather similar. In Figure 3c,d, the slow weight loss process before 250ºC is attributed to the loss of adsorbed water and interlayer water, and the weight losses are 10 wt.% and 12 wt.%, respectively. Compared with pristine L-Asp, the intercalated materials show no remarkable endothermic peak (Figure 4c,d), which indicates that the polymerization reaction of L-Asp anions may not take place. Unlike Mg-Al-CO_3^{2-} LDH, the weight losses of losing water in intercalated LDHs are mild. This might be related to the different force on the interlayer water molecules between them. Dehydroxylation of the LDH interlayer and the combustion of intercalated L-aspartic acid anions occur in the temperature range 390–430ºC. The corresponding exothermic peaks are observed at 433ºC (Figure 4c) and 435ºC (Figure 4d), respectively. The results of TG and DTA are evidence for the intercalation of L-Asp into LDH.

The chemical composition of L-Asp LDHs

The results of elemental analysis of Sample 1 are Mg, 21.24%; Al, 11.83%; C, 9.87%; N, 4.22%; H, 3.88% and those of Sample 2 are Mg, 23.07%; Al, 12.02%; C, 7.86%; N, 2.48%; H, 4.13%. Theoretical and experimental compositions of L-Asp LDHs are displayed in Table 2.

The experimentally determined Mg/Al molar ratio of L-Asp LDHs is approximately equal to that of Mg/Al input. The Mg/Al molar ratio of Sample 2, however, is little larger than that of Sample 1. This is because the pH value during the ageing process of Sample 2 is greater than that of Sample 1, resulting in enriched Mg deposited in the host layers of Sample 2. It can be

Table 2. Compositional data for synthesized LDH materials.

Sample	Chemical composition	Mg/Al molar ratio
Sample 1*	$Mg_4Al_2(OH)_{12}(C_4H_6NO_4)_2{\cdot}4H_2O$	2.0:1.0
Sample 2*	$Mg_4Al_2(OH)_{12}(C_4H_5NO_4){\cdot}4H_2O$	2.0:1.0
Sample 1**	$Mg_{4.04}Al_{2.00}(OH)_{12.08}(C_4H_6NO_4)_{0.94}(NO_3)_{1.06}{\cdot}2.92H_2O$	2.0:1.0
Sample 2**	$Mg_{4.28}Al_{2.00}(OH)_{12.56}(C_4H_5NO_4)_{0.64}(NO_3)_{0.52}{\cdot}3.50H_2O$	2.1:1.0

*: theoretical composition
**: experimental composition

https://doi.org/10.1346/CCMN.2004.0520105 Published online by Cambridge University Press

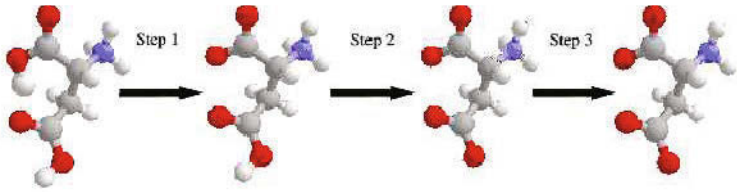


Figure 5. The ionization of L-Asp in water.

seen from Table 2 that there are co-intercalated nitrate ions within the gallery space of both samples, which is in accordance with the result of XRD (Figure 1).

Structure model of L-Asp LDHs

As shown in Table 1, the basal spacings of Sample 1 and Sample 2 are different, which might be due to the different valence states and orientations of interlayer anions. The ionization of L-Asp includes three steps in water as illustrated in Figure 5, due to the two carboxyl groups and one amido group in its structure.

The values of pKa are: pKa_1 = 1.88 (α–COOH), pKa_2 = 3.65 (R–COOH), pKa_3 = 9.60 (α–NH_3^+), respectively (Wang, 2001). Taking into account the solution pH and pKa, the distribution coefficient δ can be calculated.

Based on the experimental conditions for Sample 1 with the ageing pH at 10.0, the values of calculated δ are $\delta_1 = 3.50 \times 10^{-6}\%$, $\delta_2 = 99.7\%$, and $\delta_3 = 0.20\%$, thus L-Asp exists mainly as monovalent anion $^-OOCCHNH_3^+CH_2COO^-$ in solution during the ageing process. The d_{003} of Sample 1 is 0.93 nm. As the thickness of the LDH hydroxide basal sheet is 0.48 nm (Wykoff, 1963), the basal spacing of Sample 1 is calculated to be 0.45 nm. In the case of Sample 2, the added alkali was significantly higher, and the solution pH was 12.5 during ageing. The values of calculated δ at $\delta_1 = 1.77 \times 10^{-5}\%$, $\delta_2 = 0.40 \times 10^{-3}\%$, and $\delta_3 = 99.9\%$, result in the L-Asp existing mainly as a bivalent anion $^-OOCCHNH_2CH_2COO^-$ under this specific experimental condition. The basal spacing of Sample 2 is 0.76 nm. The covalent radius of the L-asp molecule is 0.74 nm, which is approximately equal to the experimental value of basal spacing of Sample 2. As L-Asp contains two negative charges in Sample 2, it might stand vertically in the interlayer region due to the electrostatic force between the carboxylic groups and the host layers, as depicted in Figure 6b. The basal spacing of Sample 1 is smaller than the covalent radius of the L-Asp molecule, which suggests that L-Asp might exist obliquely to the interlayer. The attraction between $-NH_3^+$ and the adjacent $-COO^-$ as well as the repulsion between $-NH_3^+$ and the host layers lead to the oblique orientation of L-Asp in Sample 1, as shown in Figure 6a, in which the oblique angle is ~40° between the host layer and the L-Asp molecular chain. The remaining positive charge of the LDH basal layer is thought to be neutralized by

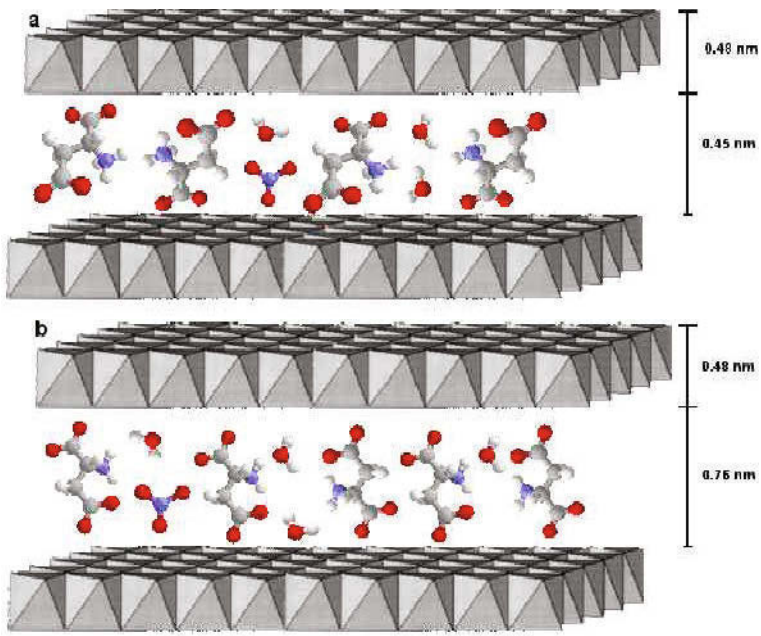


Figure 6. Schematic models of L-Asp LDHs: (a) Sample 1, and (b) Sample 2.

https://doi.org/10.1346/CCMN.2004.0520105 Published online by Cambridge University Press

Table 3. Optical activity of L-Asp, Sample 1 and Sample 2.

Sample	α (°)	$\alpha^{20}_{589.3}$ (°)
L-Asp	+0.981	+22.13
L-Asp in Sample 1	+1.390	+25.74
L-Asp in Sample 2	+0.882	+22.52

the coexistent NO_3^- ion within the gallery spaces. Whilton *et al.* (1997) reported that the gallery spacing was ~0.63 nm for aspartate LDHs, which is between the value of our results in Sample 1 (0.45 nm) and Sample 2 (0.76 nm). We compared Whilton's (1997) reaction conditions with ours, and found that the pH of the reaction mixture was ~11.5–12 in their experiment, just between our conditions of Sample 1 (pH = 10.0) and Sample 2 (pH = 12.5). Under their pH conditions, univalent anions coexist with bivalent anions in the gallery spaces of the LDH. As a result, the orientation of aspartic acid anions would be very complex, and would be a mixture of our two extreme states.

Optical activity of L-Asp LDHs

It is well known that racemization of chiral substances occurs easily, so it is essential to determine whether or not the optical activity of L-Asp is retained during intercalation. The optical rotation of L-Asp and L-Asp LDHs were measured by polarimetry. As optical rotation α is related to the length of sample tube, the solution pH and concentration, the wavelength of lamp, the measurement temperature and the type of solvent, these factors were maintained constant during measurement.

The optical rotation α and specific optical rotation $\alpha^{20}_{589.3}$ of L-Asp and L-Asp LDHs are listed in Table 3. It can be seen that the $\alpha^{20}_{589.3}$ values of Sample 1 and Sample 2 are approximately identical with that of pure L-Asp, indicating that the optical activity of L-Asp is retained during the intercalation. The small difference between them might be due to the influence of other electrolytes (such as Mg^{2+} and Al^{3+}) in the solution used for dissolving L-Asp LDHs. A study of the optical stability of intercalated L-Asp is under way in our laboratory.

CONCLUSIONS

L-Asp was intercalated into LDH by the method of coprecipitation. Two kinds of L-Asp LDHs with different basal spacings were obtained under different solution pH during the ageing process, which indicates that the solution pH during ageing has a strong influence on the structure of products. Monovalent or bivalent L-Asp anions intercalated into LDHs with different guest anion orientations can be obtained by control of the reaction conditions. Analysis by TG and DTA shows that the transformation of intercalated L-Asp is different from that of its pristine form. The optical activity of L-Asp was retained after intercalation, therefore the intercalation of chiral substances into LDH may have a potential application in the storage and transportation of biologically important chiral materials.

ACKNOWLEDGMENTS

This project was supported by the National Nature Science Foundation of China (No. 90206004).

REFERENCES

Aisawa, S., Takahashi, S., Ogasawara, W., Umetsu, Y. and Narita, E. (2001) Direct intercalation of amino acids into layered double hydroxides by coprecipitation. *Journal of Solid State Chemistry*, **162**, 52–62.

Allmann, R. (1968) The crystal structure of pyroaurite. *Acta Crystallographica Section B: Structural Crystallography and Crystal Chemistry*, **24**, 972–977.

Ambrogi, V., Fardella, G., Grandolini, G. and Perioli, L. (2001) Intercalation compounds of hydrotalcite-like anionic clays with anti-inflammatory agents – I. Intercalation and in vitro release of ibuprofen. *International Journal of Pharmaceutics*, **220**, 23–32.

Andersson, S. and Johansson, A.M. (1995) Chiral discrimination: A report on the 5th International Symposium on Chiral Discrimination held in Stockholm. *Trends in Analytical Chemistry*, **14**, VII–VIII.

Bonnet, S., Forano, C., de Roy, A., Besse, J.P., Maillard, P. and Momenteau, M. (1996) Synthesis of hybrid organo-mineral materials: anionic tetraphenylporphyrins in layered double hydroxide. *Chemistry of Materials*, **8**, 1962–1968.

Constantino, V.R.L. and Pinnavaia, T.J. (1994) Structure-reactivity relationships for basic catalysts derived from a $Mg^{2+}/Al^{3+}/CO_3^{2-}$ layered double hydroxide, *Catalysis Letters*, **23**, 361–368.

Corma, A., Fornes, V., Rey, F., Cervilla, A., Llopis, E. and Ribera, A. (1995) Catalytic air oxidation of thiols mediated at a $Mo(VI)O_2$ complex center intercalated in a Zn(II)-Al(III) layered double hydroxide host. *Journal of Catalysis*, **152**, 237–242.

Dimotakis, E.D. and Pinnavaia, T.J. (1990) New route to layered double hydroxides intercalated by organic anions: precursors to polyoxometalate-pillared derivatives. *Inorganic Chemistry*, **29**, 2393–2394.

Fogg, A.M., Dunn, J.S., Shyu, S.G., Cary, D.R. and O'Hare, D. (1998) Selective ion-exchange intercalation of isomeric dicarboxylate anions into the layered double hydroxide $[LiAl_2(OH)_6]Cl{\cdot}H_2O$. *Chemistry of Materials*, **10**, 351–355.

Fogg, A.M., Green, V.M. Harvey, H.G. and O'Hare, D. (1999) New separation science using shape-selective ion exchange intercalation chemistry. *Advanced Materials*, **11**, 1466–1469.

Fudala, A., Palinko, I., Hrivnak, B. and Kiricsi, I. (1999a) Amino acid-pillared layered double hydroxide and montmorillonite. *Journal of Thermal Analysis and Calorimetry*, **56**, 317–322.

Fudala, A., Palinko, I. and Kiricsi, I. (1999b) Preparation and characterization of hybrid organic-inorganic composite materials using the amphoteric property of amino acids: amino acid intercalated layered double hydroxide and montmorillonite. *Inorganic Chemistry*, **38**, 4653–4658.

Ingram, L. and Taylor, H.F.W. (1967) The crystal structures of sogrenite and pyroaurite. *Mineralogical Magazine*, **36**, 65–479.

Kathleen, A.C., Athanasios K. and Steven, L.S. (1988) Layered double hydroxides (LDHs). *Solid States Ionics*, **26**, 77–86.

https://doi.org/10.1346/CCMN.2004.0520105 Published online by Cambridge University Press

Manasse, E. (1919) Enargite from Calabona (Sardinia). *Attitude Society Toscana Science Nation*, **32**, 113–128.

Moujahid, E.M., Besse, J.P. and Leroux, F. (2002) Synthesis and characterization of a polystyrene sulfonate layered double hydroxide nanocomposite. *In-situ* polymerization *vs.* polymer incorporation. *Journal of Materials Chemistry*, **12**, 3324–3330.

Nakamoto, K. (1997) *Infrared and Raman Spectra of Inorganic and Coordination Compounds*, 5th edition. Wiley & Sons, New York.

Nijis, H., Clearfield, A. and Vansant, E.F. (1998) The intercalation of phenylphosphonic acid in layered double hydroxides. *Microporous and Mesoporous Materials*, **23**, 97–108.

Ogawa, M. and Kuroda, K. (1995) Photofunctions of intercalation compounds *Chemical Reviews*, **95**, 399–438.

Oriakhi, C.O., Farr, I.V. and Lerner, M.M. (1996) Incorporation of poly (acrylic acid), poly (vinylsulfonate) and poly (styrenesulfonate) within layered double hydroxides. *Journal of Materials Chemistry*, **6**, 103–107.

Oriakhi, C.O., Farr, I.V. and Lerner, M.M. (1997) Thermal characterization of poly (styrene sulfonate)/layered double hydroxide nanocomposites. *Clays and Clay Minerals*, **45**, 194–202.

Prevot, V., Forano, C. and Besse, J.P. (1998) Syntheses and thermal and chemical behaviors of tartrate and succinate intercalated Zn_3Al and Zn_2Cr layered double hydroxides. *Inorganic Chemistry*, **37**, 4293–4301.

Sels, B., Vos, D.D., Buntinx, M., Pierard, F.A., Mesmaeker, K.D. and Jacobs, P. (1999) Layered double hydroxides exchanged with tungstate as biomimetic catalysts for mild oxidative bromination, *Nature*, **400**, 855–857.

Stecher, H., Hermetter, A. and Faber, K. (1998) Mandelate racemese assayed by polarimetry. *Biotechnology Techniques*, **12**, 257–261.

Tagaya, H., Sato, S., Kuwahara, T. and Kadokawa, J.I. (1994) Photoisomerization of indolinespirobenzopyran in anionic clay matrices of layered double hydroxides. *Journal of Materials Chemistry*, **4**, 1907–1912.

Tagaya, H., Ogata, A., Kuwahara, T., Ogata, S., Karasu, M., KadoKawa, J. and Chinba, K. (1996) Intercalation of colored organic anions into insulator host lattices of layered double hydroxides. *Microporous Materials*, **7**, 151–158.

Toshiyuki, H., Yasumasa, Y., Katsunori, K. and Arsumu, T. (1995) Decarbonation behavior of Mg-Al-CO_3 hydrotalcite-like compounds during heat treatment. *Clays and Clay Minerals*, **43**, 427–432.

Ukrainczyk, L., Chibwe, M., Pinnavaia, T.J. and Boyd, S.A. (1995) Reductive dechlorination of carbon tetrachloride in water catalyzed by mineral-supported biomimetic cobalt macrocycles. *Environmental Science and Technology*, **29**, 439–445.

Wang, X.C. (2001) *Biology Chemistry.* Tsinghua University, Beijing, 11 pp.

Whilton, N.T., Vickers, P.J. and Mann, S. (1997) Bioinorganic clays: synthesis and characterization of amino- and polyamino acid intercalated layered double hydroxides. *Journal of Materials Chemistry*, **7**, 1623–1629.

Wykoff, R.W.G. (1963) *Crystal Structure.* John Wiley & Sons, New York, Vol. **1**, 268 pp.

Zhao, H.T. and Vance, G.F. (1997) Intercalation of carboxymethyl-cyclodextrin into magnesium-aluminum layered double hydroxide. *Journal of the Chemical Society, Dalton Transactions*, 1961–1965.

Zhao, H.T. and Vance, G.F. (1998) Selectivity and molecular sieving effects of organic compounds by a β-cyclodextrin-pillared layered double hydroxide. *Clays and Clay Minerals*, **46**, 712–718.

Zhao, Y., Li, F., Zhang, R., Evans, D.G. amd Duan, X. (2002) Preparation of layered double hydroxide nanomaterials with a uniform crystallite size using a new method involving separate nucleation and aging steps. *Chemistry of Materials*, **14**, 4286–4291.

(*Received 12 May 2003; revised 16 September 2003; Ms. 790; A.E. James E. Amonette*)

https://doi.org/10.1346/CCMN.2004.0520105 Published online by Cambridge University Press